Journal of Optoelectronics and Advanced Materials Vol. 5, No. 3, September 2003, p. 635 - 640

FRACTAL-LIKE STRUCTURES IN THE SELF-SIMILAR CRYSTALLIZATION WITH A TWO-PHASE ZONE

D. V. Alexandrov*, S. V. Bulitcheva, M. E. Komarovski, A. P. Malygin

Department of Mathematical Physics, Urals State University, Lenin ave. 51, Ekaterinburg, 620083, Russia

In the case of the self-similar regime in time-dependent crystallization, the spatial coordinate, ξ, set along the solidification direction and time t are connected by means of the following relation: $\xi \sim \sqrt{t}$. This scaling relation usually takes place for crystallization regimes far from the initial stage $t = 0$ of the process. We demonstrate that nonstationary crystallization processes in the presence of the mushy region are described by means of the fractal-like power laws at initial and self-similar stages.

(Received July 10, 2003; accepted July 31, 2003)

Keywords: Fractal, Self-similar crystallization, Crystal growth

1. Introduction

Mathematical descriptions of crystallization processes play very important role in crystal growth [1,2], engineering, [3], oceanography [4] and metallurgy [5]. The transition amorphous-to-crystalline in the materials for optical phase-change memories is of great practical importance [6]. The mathematical models allow to predict many properties of solids produced by melt cooling. If the liquid is an alloy (a mixture of two or more components) its crystallization process completely differs from the solidification of a pure liquid. In particular, various distributions of impurity in the solid phase lead to different mechanical and physical properties of ingots. This phenomenon arises due to the impurity displacement into the melt by the moving front of solidification. If the impurity displacement is rather large, the constitutional supercooling originates ahead of the planar solid-liquid interface [7] and, generally speaking, the two-phase zone (mushy region) appears. Moreover, solid nuclei in the form of newly born crystals may evolve in this zone. The authors of Ref. [8] developed a full set of thermodynamic equations for a mushy zone, and solved a mush-reduced set of them approximately for the constrained growth of a binary alloy. A more complete solution has since been given in Refs. [9,10] for the steady-state solidification conditions. Nevertheless, solidification with a constant rate is the specific regime. Generally speaking, the rate of solidification is a function of all operating and physical parameters and also it is a time dependent function. As was shown in Refs. [11] and [12], the front rate is a nearly linear function of time at the initial stage of crystallization in an ingot mold. The constitutional supercooling origination (the latter occurs when the concentration gradient $G_C = m\partial C_L/\partial\xi$ exceeds the temperature one $G = \partial\theta_L/\partial\xi$ at the planar front; here m is the liquidus slope determined from the phase diagram, C_L and θ_L are the concentration and temperature fields in the liquid phase) leads under certain circumstances to the mushy zone solidification and the classical description of crystallization by means of the planar front model becomes inapplicable. However, if the process is far from the cooled wall and the constitutional supercooling and/or a mushy layer are absent, solidification with a planar front proceeds in unsteady-

* Corresponding author: Dmitri.Alexandrov@usu.ru

state manner and after a lapse of time the process approaches to own self-similarity. Such a scenario of crystallization was experimentally studied in Ref. [13] on the basis of aqueous solution of sodium nitrate. At first, solidification proceeds within the framework of the Stefan thermodiffusion problem with a planar front. Further, after a lapse of time the planar shape of the solid-liquid interface is destroyed and solidification is described with the help of the mushy layer model [13]. The governing set of equations and boundary conditions for the mushy layer (see Ref. [13]) is essentially nonlinear. Therefore, in Ref. [13], this set is solved only numerically for two binary mixtures. The present study is concerned with approximate power solutions of the self-similar model with the thermodynamically equilibrium two-phase zone. We demonstrate that the bulk fraction of the solid phase and impurity concentration are described by fractal-like (scaling) laws.

2. Mathematical description

Let us consider a unidirectional solidification process of a binary melt or solution directed along the ξ axis. The cooled wall is placed at $\xi = 0$ and regions $0 < \xi < \Sigma_S(t)$ and $\Sigma_L(t) < \xi < \infty$ are filled with the solid and liquid phases whereas the region $\Sigma_S < \xi < \Sigma_L$ is occupied with the two-phase zone (Σ_S and Σ_L stand for the solid phase – two-phase zone and two-phase zone – liquid phase coordinates). The temperature and concentration fields in pure liquid and solid phases are governed by the following parabolic-type equations

$$\frac{\partial \theta_L}{\partial t} = a_L \frac{\partial^2 \theta_L}{\partial \xi^2}, \qquad \frac{\partial C_L}{\partial t} = D_L \frac{\partial^2 C_L}{\partial \xi^2}, \quad \Sigma_L(t) < \xi < \infty, \tag{1}$$

$$\frac{\partial \theta_S}{\partial t} = a_S \frac{\partial^2 \theta_S}{\partial \xi^2}, \qquad \frac{\partial C_S}{\partial t} = D_S \frac{\partial^2 C_S}{\partial \xi^2}, \quad 0 < \xi < \Sigma_S(t). \tag{2}$$

Here θ_S and C_S are the temperature and concentration in the solid, a_L and a_S are the thermal diffusivities in the liquid and solid, D_L and D_S are the diffusion coefficients in these phases. The heat and mass transfer processes in the mushy region are governed by the following equations

$$\frac{\partial}{\partial t}(\rho_m c_m \theta_m) = \frac{\partial}{\partial \xi}\left(K_m \frac{\partial \theta_m}{\partial \xi}\right) + L_V \frac{\partial \varphi}{\partial t}, \frac{\partial}{\partial t}((1-\varphi)C_m) = \frac{\partial}{\partial \xi}\left(D_m \frac{\partial C_m}{\partial \xi}\right) - kC_m \frac{\partial \varphi}{\partial t}, \Sigma_S < \xi < \Sigma_L, \tag{3}$$

where θ_m and C_m are the temperature and concentration fields in the mushy zone, φ is the bulk fraction of the solid in this zone, and

$$\rho_m c_m(\varphi) = \rho_L c_L(1-\varphi) + \rho_S c_S \varphi, \; K_m(\varphi) = K_L(1-\varphi) + K_S\varphi, \; D_m(\varphi) = D_L(1-\varphi) + D_S\varphi.$$

Here ρ_L and ρ_S are the densities in the solid and liquid, $c_L = K_L/\rho_L a_L$ and $c_S = K_S/\rho_S a_S$ are the thermal capacities in these phases. The two-phase zone is assumed to be in a state of thermodynamic equilibrium. This means that the temperature in both of the phases is equal to the phase transition temperature connected with the solute concentration. Let us write down the liquidus equation in a linear form, i.e.

$$\theta_m = \theta_0 + mC_m, \qquad \Sigma_S < \xi < \Sigma_L. \tag{4}$$

The set (1) - (4) must be supplemented by the boundary conditions imposed at both interfaces. Namely

$$\varphi = \varphi_*,\ K_S \frac{\partial \theta_S}{\partial \xi} - K_m \frac{\partial \theta_m}{\partial \xi} = L_V (1-\varphi_*) \frac{\partial \Sigma}{\partial t},\ C_S = kC_m,\ \xi = \Sigma_S, \tag{5}$$

$$(1-k)(1-\varphi_*) C_m \frac{\partial \Sigma_L}{\partial t} + D_m \frac{\partial C_m}{\partial \xi} = 0, \quad \theta_m = \theta_S, \xi = \Sigma_S, \tag{6}$$

$$\varphi = 0, C_m = C_L, \quad D_m \frac{\partial C_m}{\partial \xi} = D_L \frac{\partial C_L}{\partial \xi}, \quad \theta_m = \theta_L, \quad K_m \frac{\partial \theta_m}{\partial \xi} = K_L \frac{\partial \theta_L}{\partial \xi}, \quad \xi = \Sigma_L, \tag{7}$$

where K_S and K_L are the thermal conductivities in the solid and liquid, L_V is the latent heat parameter (per unit volume), k is the equilibrium partition coefficient, θ_0 is the phase transition temperature for the pure matter.

Temperature and concentration fields at the cooled wall and far from the front in the liquid will be regarded as known, i.e.

$$\theta_S = \theta_W, \quad C_S = C_W = kC_{L\infty}, \quad \xi = 0, \tag{8}$$

$$\theta_L \to \theta_{L\infty}, \quad C_L \to C_{L\infty}, \quad \xi \to \infty. \tag{9}$$

3. Results and conclusions

In the case of self-similar crystallization the spatial coordinate ξ and time t are connected by the relation $x \equiv (\xi - \Sigma_S)/2\sqrt{D_L t}$ while the solid-mushy Σ_S and mushy-liquid Σ_L boundaries are expressed as (Ref. [14]) $\Sigma_S = 2\lambda_S \sqrt{D_L t}$ and $\Sigma_L = 2\lambda_L \sqrt{D_L t}$, where constants λ_S and λ_L are solutions of the aforementioned model. Further, we demonstrate that solutions of the model (1)-(9) strengthen a hypothesis about self-similar distributions of the bulk fraction φ and the solute concentration C_m. It is well-known that many fractal objects met in nature are described by means of scaling laws [15,16]. Moreover, the fractal-like structure of the steady-state mushy zone was observed in Ref. [17]. Taking into account the latter we describe the self-similar mushy zone by fractal-like power laws in the spirit of Ref. [17]. Let us introduce the following homogeneous self-similar functions for the bulk fraction φ and concentration C_m in the two-phase zone [17]:

$$\varphi(y) = \varphi_* y^D, \quad C_m(y) = C_{m\varepsilon} + (C_{m*} - C_{m\varepsilon}) y^D, \quad y = 1 - \frac{x}{\varepsilon}, \quad \varepsilon = \lambda_L - \lambda_S, \tag{10}$$

where C_{m*} and $C_{m\varepsilon}$ are the concentrations at the boundaries solid phase – two-phase zone and two-phase zone – liquid phase. Expressions (10) satisfy to the scaling relations

$$\varphi(\lambda y) = \lambda^D \varphi(y),\ C_m(\lambda y) - C_{m\varepsilon} = \lambda^D (C_m(y) - C_{m\varepsilon}).$$

Here λ is a constant. The scaling parameter D plays the role of dimensions for fractal objects [15]. It is easy to see that the value of $C_{m\varepsilon}$ is not a fractal-like part of the function $C_m(y)$. Apparently, this is due to the fact that the boundary two-phase zone – liquid phase does not displace the solute concentration into the pure liquid phase. Substituting the self-similar variables introduced above in the set (1)-(9) we get the set of ordinary differential equations supplemented by the boundary conditions (see, for example, Ref. [14]). The nonlinear set of equations obtained in this way is solved numerically. Since the procedure of numerical solutions is quite standard, we will not dwell on this point. The results in the planes of (φ, x) and (C_m, x) are illustrated in Figs. 1 and 2 for two sets given in Table 1 (all temperatures are measured from the point $\theta_0 = 0\ ^{\circ}$C; symbols 1 and 2 near the curves correspond to sets I and II respectively). Further, we approach the exact numerical results by means of the scaling relations (10) (values of φ_*, C_{m*} and $C_{m\varepsilon}$ are known from numerical solutions of the

model). These results are illustrated in Figs. 1 and 2 by symbols "+". It is easy to see that power laws (10) are in a good agreement with numerical solution.

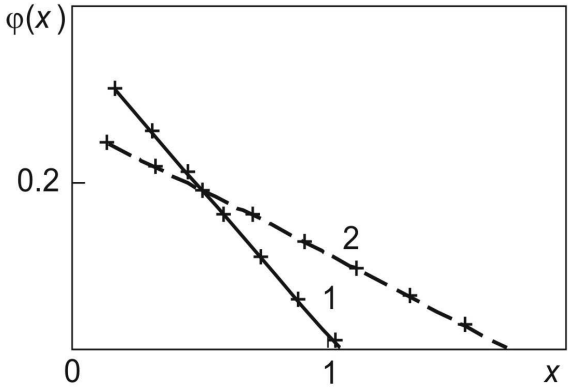

Fig. 1. The bulk fraction of the solid phase as a function of spatial coordinate within the two-phase zone. (1): $\lambda_S = 0.154$, $\lambda_L = 1.05$, $\varphi_* = 0.328$, $D = 1.03$,(2): $\lambda_S = 0.154$, $\lambda_L = 1.74$, $\varphi_* = 0.239$, $D = 1.07$.

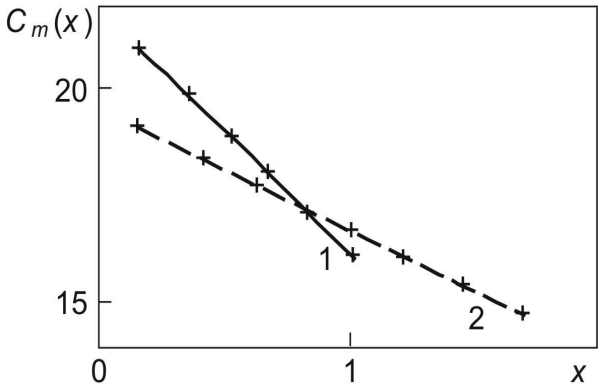

Fig. 2. The solute concentration as a function of spatial coordinate within the two-phase zone. (1): $\lambda_S = 0.154$, $\lambda_L = 1.05$, $\sigma_* = 20.952$, $D = 1.03$, (2): $\lambda_S = 0.154$, $\lambda_L = 1.74$, $\sigma_* = 19.281$, $D = 1.07$.

Table 1. Parameter values used for the two sets of results in accordance with Refs. [13,14].

Property	Set I	Set II: $NaNO_3$+H_2O	Units
Thermal conductivity, K_L	$1.3 \cdot 10^{-3}$	1.3×10^{-3}	cal/(cm·s·^{O}C)
Thermal conductivity, K_S	$1.3 \cdot 10^{-3}$	5.3×10^{-3}	cal/(cm·s·^{O}C)
Thermal diffusivity, a_L	$1.3 \cdot 10^{-3}$	1.3×10^{-3}	cm^2/s
Thermal diffusivity, a_S	$1.3 \cdot 10^{-3}$	1.2×10^{-2}	cm^2/s
Diffusion coefficient, D_L	$1.0 \cdot 10^{-5}$	1.0×10^{-5}	cm^2/s
Diffusion coefficient, D_S	$1.0 \cdot 10^{-9}$	1.0×10^{-9}	cm^2/s
Latent heat parameter, L_V	80	73.6	cal/cm^3
Liquidus slope, m	-0.4	-0.4	^{O}C
Segregation coefficient, k	0	0	-
Liquid phase density, ρ_L	1.0	1.0	g/cm^3
Solid phase density, ρ_S	1.0	0.48	g/cm^3
Initial concentration, $C_{L\infty}$	14	14	-
Temperature, $\theta_{L\infty}$	15	15	^{O}C

Let us especially emphasize that the bulk fraction and solute concentration profiles within the two-phase zone are determined only by means of boundary values φ_*, C_{m*} and $C_{m\varepsilon}$. Moreover, in the case of fixed physical and operating parameters, these profiles are independent on the scaling parameter D, which is equal to 1.03 ± 0.05 and 1.07 ± 0.05 for sets I and II respectively. This result is in a good agreement with Ref. [16], where similar analyses are carried out for the steady-state solidification with a mushy layer (authors of Ref. [17] have found that the scaling parameter D varies from 1 to 2). Since the self-similar solutions describe nonstationary solidification far from its initial

stage ($t = 0$), it is of interest to study how the scaling relations (10) work at initial stages (near the vicinity $t = 0$). In order to study the latter let us pay our attention to experiments of Ref. [18]. Fig. 3 demonstrates distributions of the solute concentration ahead of the boundary solid phase – two-phase zone, $x = 0$, for initial stages of nonstationary crystallization of the set KCl (here x and ε play the role of dimensional variables). The constitutional supercooling arises (and, as a consequence, the two-phase zone originates) for crystallization time $t > 60$ s. As is seen from Fig. 3, the concentration profile approaches to some invariable self-similar distribution with increasing in time (in other words, a distance between neighboring curves decreases). Further, we compare the scaling relation (10) with experimental data in Fig. 3. The scaling parameter D is of the order of 2.7 for all curves in Fig. 3, i.e. for different solidification time. Practically it means that experiments of Ref. [18] strengthen a hypothesis about a fractal structure of the two-phase zone solidified in nonstationary manner at initial stages of the process.

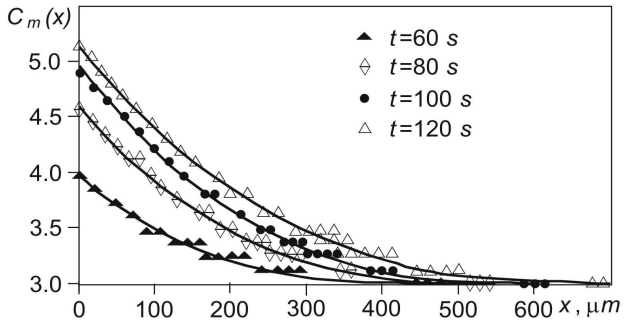

Fig. 3. The solute concentration in the two-phase zone as a function of the spatial coordinate (symbols – experiments of Ref. [18], solid curves – calculations in accordance with relation (10)).

4. Conclusions

It was revealed a fractal-like structure of the two-phase zone for nonstationary crystallization regimes at initial and self-similar stages of the process.

The fractal-like scaling laws (10) are in a good agreement with numerical calculations and experimental data.

Acknowledgements

This work was made possible in part by Award No. REC-005 of the U.S. Civilian Research and Development Foundation for the Independent States of the Former Soviet Union and due to the financial support of grants Nos. 01-02-96430Ural, 02-03-96437Ural (Russian Foundation for Basic Research), MD-336.2003.02 (President of Russian Federation Grant) and E02-4.0-86 (Minobrazovanie RF). One of the authors, Dmitri Alexandrov, is grateful to the Basic Research and Higher Education Program for the financial support of young scientists.

References

[1] R. A. Laudise, The Growth of Single Crystals, Prentice Hall, New York (1972).
[2] J. C. Brice, The Growth of Crystals from Liquid, North Holland, Amsterdam (1973).
[3] F. Rosenberg, Fundamentals of Crystal Growth, Vol. 1, Springer, Berlin (1979).
[4] P. V. Hobbs, Ice Physics, Clarendon, Oxford, (1974).

[5] B. Chalmers, Principles of Solidification, Wiley, New York (1964).
[6] E. Morales-Sánchez, J. González-Hernández, E. Prokhorov, J. Optoelectron. Adv. Mater. **3**(2), 333 (2001).
[7] J. S. Langer, Rev. Mod. Phys. 52, 1 (1980).
[8] R. N. Hills, D. E. Loper, P. H. Roberts, Q .J. Appl. Math. 36, 505 (1983).
[9] D. V. Alexandrov, J. Crystal Growth **222**, 816 (2001).
[10] D. V. Alexandrov, Acta Mater. **49**, 759 (2001).
[11] D. V. Alexandrov, A. G. Churbanov, P. N. Vabishchevich, Int. J. Fluid Mech. Res. **26**, 248 (1999).
[12] D. V. Alexandrov, Int. J. Fluid Mech. Res. **27**, 223 (2000).
[13] H. E. Huppert, M. G. Worster, Nature **314**, 703 (1985).
[14] M. G. Worster, J. Fluid Mech. **167**, 481 (1986).
[15] J. Feder, Fractals, Plenum Press, New York (1988).
[16] B. B. Mandelbrot, Fractal Geometry of Nature, Freeman, New York (1982).
[17] D. V. Alexandrov, A. O. Ivanov, Doklady Physics **47** (7), 499 (2002).
[18] K. Nagashima, Y. Furukawa, J. Crystal Growth **209**, 167 (2000).